ISSN: 0067-2904

Modeling and Analysis of a Prey-Predator System Incorporating Fear, Predator-Dependent Refuge, with Cannibalism in Prey

Ahmed Sami Abdul ghafour[1]*, Raid Kamel Naji[2]
[1] *Scientific Affairs Department, Al-Iraqia University, Baghdad, Iraq*
[2]*Department of Mathematics, College of Science, University of Baghdad, Baghdad, Iraq*

Received: 17/11/2022 Accepted: 27/2/2023 Published: 30/1/2024

Abstract

The relationship between prey and predator populations is hypothesized and examined using a mathematical model. Predation fear, cannibalism among the prey population, and a refuge reliant on predators are predicted to occur. This study set out to look at the long-term behavior of the proposed model and the effects of its key elements. The solution properties of the model were investigated. All potential equilibrium points' existence and stability were looked at. The system's persistence requirements were established. What circumstances could lead to local bifurcation near equilibrium points was uncovered. Suitable Lyapunov functions are used to study the system's overall dynamics. Numerical simulations were conducted to verify the model's derived long-term behavior and understand the implications of the model's primary parameters in order to support the analytical conclusions. It is observed that the system undergoes different types of local bifurcation including Hopf bifurcation.

Keywords: prey-predator; prey cannibalism; a refuge; fear; stability, bifurcation

نمذجة وتحليل نظام الفريسة المفترس الذي يدمج الخوف والملجأ المعتمد على المفترس والافتراس الذاتي في الفريسة

احمد سامي عبد الغفور[1]*, رائد كامل ناجي[2]
[1]قسم الشؤون العلمية، الجامعة العراقية، بغداد، العراق
[2]قسم الرياضيات، كلية العلوم، جامعة بغداد، بغداد، العراق

الخلاصة

في هذا البحث تم اقتراح العلاقة بين الفريسة والمفترس وتحليلها من خلال استخدام نموذج رياضي. ويدرس هذا النموذج تأثير الخوف للفريسة من الافتراس والملجأ الذي يعتمد على الحيوانات المفترسة وظاهرة الافتراس الذاتي بين الفرائس. تهدف هذه الدراسة إلى النظر في السلوك طويل الأجل للنموذج المقترح وآثار عناصره الرئيسية. تم التحقيق في خصائص الحل للنموذج. تم النظر في وجود واستقرار جميع نقاط التوازن المحتملة. وتحديد متطلبات استمرار النظام. وتم الكشف عن الظروف التي يمكن أن تؤدي إلى تشعب محلي بالقرب من

* Email: alania961@gmail.com

نقاط التوازن. واستخدام دالة ليابانوف المناسبة لدراسة الديناميكيات العامة للنظام. تم إجراء عمليات محاكاة عددية للتحقق من السلوك طويل الأجل المشتق من النموذج وفهم الآثار المترتبة على المعلمات الأساسية للنموذج من أجل دعم الاستنتاجات التحليلية. ويلاحظ أن النظام يخضع لأنواع مختلفة من التشعب المحلي بما في ذلك تشعب هوبف

1. Introduction

Less attention is paid to the dynamics of predator-prey interactions when the predator uses other survival strategies due to a lack of food supplies, with the majority of studies in mathematical ecology focusing on the direct predation of prey species. The Lotka-Volterra model, which was initially published separately by Lotka and Volterra, is currently used to describe interactions between prey and predators [1]. Consuming a member of the same species as food is cannibalism. A typical intraspecific interaction that occurs in both aquatic and terrestrial populations is cannibalism [2]. Cannibalism rates rise in areas with insufficient nutrition because people turn to other members of their own species for additional sustenance. Cannibalism controls population growth by reducing possible competition for resources like food, shelter, and territory, which makes them more accessible. It has been demonstrated that the prevalence of cannibalism lowers the predicted survival rate of the entire group and raises the chance of consuming a relative, despite the fact that it may benefit the individual. As the frequency of encounters between hosts rises, there may be additional detrimental impacts, such as an increased risk of disease transmission. Cannibalism, however, does not as was formerly thought only occur in extreme food shortages or under artificial or unnatural conditions; it can also happen in a number of species under natural circumstances [3]. Accordingly, cannibalism can occur in both the species' prey as well as predator.

It follows that there are significant differences between the studies on various types of predator-prey interactions and that on the classic predator-prey paradigm. However, Deng et al. [4] discovered that prey species with a significant rate of cannibalism help them survive in the environment and that predator species with a bigger quantity of this cannibalism propensity are the primary causes of prey extinction. Zhang and his coauthors found system dynamics to be significantly impacted by cannibalism and profit from cannibalism factors [5]. The stability of the system changes numerous times when the cannibalism parameter fluctuates around the coexistence steady state, but when there is considerable cannibalism, the system stabilizes globally. A mathematical model that incorporates predator cannibalism and refuge was recently considered by Rayungsari et al [6] to explain the interplay between predator and prey. To describe food transmission, they used the Lotka-Volterra type of functional response. However, the authors of [7] created and examined a mathematical model that takes predator cannibalism and refuge into account to characterize the interaction between predator and prey. They made the assumption that the population of prey contains both predator-dependent refuge and predation fear.

In addition to cannibalism, the predator-prey interaction is also interesting to examine because of the prey's tendency to hide from capture and attack by the predator. Ecologically speaking, this behavior is referred to as refuge. Our understanding of the dynamic connection between prey and predator has improved as a result of the development of analytical techniques and computerization, which have increasingly supplied a more accurate representation of ecological systems. A key component of predator-prey systems has been the hiding behavior of the prey, and the effects of this behavior on stability have been examined in many models. Prey that cannot be killed by predators in a fixed proportion or number is how refuge has traditionally been introduced. The utilization of refuges by prey may have a stabilizing influence on predator-

prey dynamics, according to some early theoretical studies; however, other models do not exhibit this straightforward pattern [8]–[12]. Only a few studies [13]–[15] have used a predator-prey model system with prey refuge proportional to both species. Even still, taking into account prey refuge proportional to both species brings our model system closer to reality since, in some natural systems, prey refuge may be impacted by both the number of predators and prey.

Later, a number of studies concentrated on and investigated the effect of a new kind of predator's impact (one that does not kill) on prey populations [16]–[21] and the references therein. This effect, which reduces the prey birth rate, is known as fear in prey individuals. Predator-induced fear keeps prey animals out of open settings, denying them the freedom to carry out regular activities like mating. As a result, their capacity for reproduction is decreased by their fear of predators. It is critical to consider the price of fear as a decrease in reproduction. Wang et al. [16] published a prey-predator model that took into account the effect of fear on prey reproduction. Additionally, it was explained how a high level of fear may stabilize the system by ruling out the possibility of periodic fixes. Furthermore, Panday et al. [17] examined how fear affected a Holling type-II functional response in a tri-trophic food chain model. Since the system displays chaotic behavior for smaller values of both of these variables, they came to the conclusion that chaotic oscillations may be controlled by increasing the fear parameters. A prey refuge is a great way to reduce the possibility that predators may use their victim's biomass excessively.

In contrast to the above studies, in this paper, predation fear, predator-dependent refuge, and cannibalism in the prey population are formulated and studied.

2. Model Formulation

The practice of eating another member of the same species as food is known as cannibalism. In the animal kingdom, cannibalism is a typical ecological relationship. Therefore, a mathematical formulation of an ecological system with a prey-predator incorporating cannibalism in prey species is presented in this section. The model has considered both the predator-dependent refuge and the fear of predation. Furthermore, Holling type II's functional response serves as a representation of the predation process. In fact, fear affects the prey's birth rate and makes the prey's refuge depend on the predator since the intensity of predation inhibits the prey's population from mating properly and causes them to hide in various shelters. Accordingly, the dynamic of the above prey-predator system can be described mathematically in the following set of nonlinear first-order autonomous differential equations.

$$\begin{aligned}\frac{dX}{dT} &= X\left(\frac{r}{1+fY} - d_1 - bX + a_3 - \frac{a_1(1-cY)Y}{K_1+X(1-cY)} - \frac{eX}{K_2+X}\right) = Xf_1(X,Y) = F_1(X,Y)\\ \frac{dY}{dT} &= Y\left(\frac{a_2X(1-cY)}{K_1+X(1-cY)} - d_2\right) = Yf_2(X,Y) = F_2(X,Y)\end{aligned} \tag{1}$$

where all the coefficients are positive constants and can be described in table (1).

It is clear from the system (1) that the interaction functions $F_1(X,Y)$ and $F_1(X,Y)$ in the right-hand side of the system (1), are continuous and have continuous partial derivatives on the domain $\mathbb{R}^2_+ = \{(X,Y) \in \mathbb{R}^2 : X \geq 0, Y \geq 0\}$. Hence, they are locally-Lipschitz functions in $\mathbb{R}^2_+$. Consequently, due to the fundamental existence and uniqueness theorem, it is obtained that system (1) with any non-negative initial condition $X(0) \geq 0$, and $Y(0) \geq 0$ there exists $T > 0$ so that the system (1) has a unique solution defined in $\mathbb{R}^2_+$.

Table 1: Variables and parameters description

Variables and Parameter	Description
$X(T)$	The population size of the prey at time T
$Y(T)$	The population size of the predator at time T
r	The prey birth rate
d_1	The prey's natural death rate
b	The prey intraspecific competition
f	The prey's fear level, which is involved in the fear function $\frac{1}{1+fY}$.
a_1	The attack rate
K_1	The half-saturation constant.
$c \in [0,1]$	The prey's refuge rate; hence the refuge amount is cXY, which leaves $X(1-cY)$ of the prey available to be hunted by the predator
a_2	The conversion rate of prey biomass into predator birth
a_3	The conversion rate of cannibalism into prey birth
d_2	The predator's natural death rate
e	The cannibalism rate in prey.
K_2	The half-saturation constant of cannibalism

3. Properties of the solution

This section treats the properties of the solution of system (1), such as positivity and bounded as shown in the following theorems.

Theorem 1. All system (1)'s solutions with initial values $(X(0), Y(0)) \in \mathbb{R}^2_+$ are non-negative.
Proof. From the equations of the system (1) with the given initial value it is clear that the solution can be written as:

$$X(t) = X(0)\exp\left[\int_0^t \left(\frac{r}{1+fY(u)} - d_1 - bX(u) + a_3 - \frac{a_1(1-cY(u))Y(u)}{K_1+X(u)(1-cY(u))} - \frac{eX(u)}{K_2+X(u)}\right)du\right]$$

Similarly,

$$Y(t) = Y(0)\exp\left[\int_0^t \left(\frac{a_2X(u)(1-cY(u))}{K_1+X(u)(1-cY(u))} - d_2\right)du\right]$$

Therefore, if $X(0) = 0$, and $Y(0) = 0$ then it is obtained that $X(t) = Y(t) = 0$ for all the time. Thus due to the positivity of the exponential function in the above two equations, it is concluded that $X(t) \geq 0$, and $Y(t) \geq 0$ indefinitely. Hence the proof is complete.
Now, before the uniformly bounded system (1)'s solution is proved, the following two lemmas given by Chen [22] are presented.

Lemma 2.1 [22]: If $a > 0, b > 0$, and $x' \geq (\leq) b - ax$, when $t \geq 0$, and $x(0) > 0$, we have

$$x(t) \geq (\leq)\frac{b}{a}\left[1 + \left(\frac{ax(0)}{b} - 1\right)e^{-at}\right].$$

Lemma 2.2 [22]: If $a > 0, b > 0$, and $x' \geq (\leq) x(b - ax^{\alpha})$, when α is a positive constant, $t \geq 0$, and $x(0) > 0$, we have

$$x(t) \geq (\leq)\left(\frac{b}{a}\right)^{1/\alpha}\left[1 + \left(\frac{bx^{-\alpha}(0)}{a} - 1\right)e^{-bat}\right]^{-1/\alpha}.$$

Theorem 2: All system (1)'s solutions that initiate in the positive quadrant are uniformly bounded.
Proof: From the first equation of system (1), it is obtained that

$$\frac{dX}{dT} \leq X(r + a_3 - d_1 - bX).$$

Therefore, by applying lemma (2.2), it is reached:

$$X(T) \leq \left(\frac{r+a_3-d_1}{b}\right)\left[1+\left(\frac{r+a_3-d_1}{b}X^{-1}(0)-1\right)e^{-(r+a_3-d_1)T}\right].$$

Therefore

$$\lim_{T\to\infty}\sup X(T) \leq \frac{r+a_3-d_1}{b} = \sigma_1.$$

Let $W = X + \frac{a_1}{a_2}Y$, then it is obtained that

$$\frac{dW}{dt} = \frac{dX}{dt} + \frac{a_1}{a_2}\frac{dY}{dt} \leq (r+a_3-d_1)X - \frac{a_1}{a_2}d_2Y \pm d_2X,$$

which gives that:

$$\frac{dW}{dt} + d_2W \leq (r+a_3+d_2-d_1)\sigma_1 = \sigma_2$$

Therefore, by applying lemma (2.1), for $T \to \infty$ it is obtained that

$$\sup W(T) \leq \frac{\sigma_2}{d_2}.$$

Hence the proof is complete.

4. Equilibrium points and stability analysis

It is clear that system (1) has two equilibrium points belonging to the boundary axes while the system has at least one positive equilibrium point in the interior of the first quadrant under the specific conditions determined below. These points can be described below.

The vanishing equilibrium point (VEP) $P_1 = (0,0)$ always exists.

The axial equilibrium point or predator-free equilibrium point (AEP) $P_2 = (m, 0)$, where m represents the positive root of the equation

$$X^2 - \frac{(r-e+a_3-d_1-bK_2)}{b}X - \frac{K_2(r+a_3-d_1)}{b} = 0. \quad (2)$$

Clearly, the term $r + a_3 - d_1$ is positive, which is known as the prey's survival condition, hence equation (2) has a unique positive root given by

$$m = \frac{(r-e+a_3-d_1-bK_2)}{2b} + \frac{1}{2}\sqrt{\left(\frac{(r-e+a_3-d_1-bK_2)}{b}\right)^2 + 4\left(\frac{K_2(r+a_3-d_1)}{b}\right)}. \quad (3)$$

Furthermore, if $r + a_3 - d_1 < 0$ then the coefficients of equation (2) do not change the sign and thus equation (2) has no positive root, which leads to the extinction of X.

The coexistence equilibrium point (COEP) $P_3 = (X^*, Y^*)$, where

$$X^* = \frac{d_2K_1}{(1-cY^*)(a_2-d_2)}. \quad (4)$$

While Y^* represents a positive root of the fifth-order polynomial equation

$$A_0Y^5 + A_1Y^4 + A_2Y^3 + A_3Y^2 + A_4Y + A_5 = 0, \quad (5)$$

where

$$A_0 = c^3fa_1K_2(a_2-d_2)^3.$$

$$A_1 = -c^2fa_1d_2K_1(a_2-d_2)^2 + c^2a_1K_2(\mathrm{c}-3f)(a_2-d_2)^3.$$

$$A_2 = a_1cK_1d_2(a_2-d_2)^2(2f-c) + 3a_1cK_2(a_2-d_2)^3(f-c) + c^2fa_2K_1K_2(a_3-d_1)(a_2-d_2)^2.$$

$$A_3 = a_1d_2K_1(f-2c)(a_2+d_2)^2 + d_2K_1^2cfa_2(e-a_3+d_1)(a_2-d_2) + a_1K_2(3c-f)(a_2-d_2)^3 + ca_2K_1K_2(a_2-d_2)^2[cr+(a_3-d_1)(c-2f)] + bcfa_2d_2K_1^2K_2(a_2-d_2).$$

$$A_4 = -a_1d_2K_1(a_2-d_2)^2 + a_2d_2K_1^2(a_2-d_2)[-cr+(c-f)(e-a_3+d_1)] - bfa_2d_2^2K_1^3 - a_1K_2(a_2-d_2)^3 - a_2K_1K_2(a_2-d_2)^2[2cr+(a_3-d_1)(2c-f)] + ba_2d_2K_1^2K_2(a_2-d_2)(c-f).$$

$$A_5 = -a_2d_2K_1^2(a_2-d_2)[(e-r)-(a_3-d_1)] - ba_2d_2^2K_1^3 + a_2K_1K_2(a_2-d_2)^2(r+a_3-d_1) - ba_2d_2K_1^2K_2(a_2-d_2).$$

Obviously, for the positivity of X^*, the following condition should be satisfied.

$$d_2 < a_2. \tag{6}$$

Moreover, since condition (6) leads to $A_0 > 0$ always, then equation (5) has a unique positive root provided that one set of the following sets of conditions holds.

$$\left.\begin{array}{l} A_1 > 0, A_2 > 0, A_4 < 0, A_5 < 0 \\ A_1 > 0, A_2 > 0, A_3 > 0, A_5 < 0 \\ A_1 > 0, A_3 < 0, A_4 < 0, A_5 < 0 \\ A_2 < 0, A_3 < 0, A_4 < 0, A_5 < 0 \end{array}\right\}. \tag{7}$$

Otherwise, equation (5) has at least one positive root provided that $A_5 < 0$.

The stability analysis of the above equilibrium points is investigated using the linearization technique. The Jacobian matrix (JM) of the system (1) at the point (X, Y) is computed in order to examine the local asymptotically stability (LAS) of each equilibrium point.

The general JM of the system (1) is given by:

$$J = \begin{bmatrix} X\frac{\partial f_1}{\partial X} + f_1 & X\frac{\partial f_1}{\partial Y} \\ Y\frac{\partial f_2}{\partial X} & Y\frac{\partial f_2}{\partial Y} + f_2 \end{bmatrix}, \tag{8}$$

where f_1 and f_2 are given in the system (1), while

$$\frac{\partial f_1}{\partial X} = -b + \frac{Y(1-cY)^2 a_1}{(X(1-cY)+K_1)^2} - \frac{eK_2}{(X+K_2)^2},$$
$$\frac{\partial f_1}{\partial Y} = -\frac{fr}{(1+fY)^2} - \frac{cXY(1-cY)a_1}{(X(1-cY)+K_1)^2} - \frac{(1-2cY)a_1}{X(1-cY)+K_1}$$
$$\frac{\partial f_2}{\partial X} = \frac{K_1(1-cY)a_2}{(X(1-cY)+K_1)^2}$$
$$\frac{\partial f_2}{\partial Y} = -\frac{K_1 cXa_2}{(X(1-cY)+K_1)^2}.$$

Accordingly, the JM at the VEP can be written as:

$$J_{P_1} = \begin{bmatrix} r - d_1 + a_3 & 0 \\ 0 & -d_2 \end{bmatrix} \tag{9}$$

Hence, the eigenvalues of J_{P_1} are given by:

$$\lambda_{11} = r - d_1 + a_3, \lambda_{12} = -d_2. \tag{10}$$

Thus, VEP is LAS if and only if the following condition is met.

$$r + a_3 < d_1. \tag{11}$$

Clearly, condition (11) leads extinction of the X and hence extinction of Y. However, the VEP is a saddle point when condition (11) is reflected.

The JM at the AEP can be determined by:

$$J_{P_2} = \begin{bmatrix} -m\left(b + \frac{eK_2}{(m+K_2)^2}\right) & -m\left(f\mathrm{r} + \frac{a_1}{m+K_1}\right) \\ 0 & \frac{ma_2}{m+K_1} - d_2 \end{bmatrix}. \tag{12}$$

Hence, the eigenvalues of J_{P_2} are given by:

$$\lambda_{21} = -m\left(b + \frac{eK_2}{(m+K_2)^2}\right), \lambda_{22} = \frac{ma_2}{m+K_1} - d_2. \tag{13}$$

Thus, AEP is LAS if and only if the following condition is met.

$$\frac{ma_2}{m+K_1} < d_2. \tag{14}$$

Otherwise, it is saddle point if the condition (14) is reflected.

The JM at the COEP can be written as follows:

$$J_{P_3} = \begin{bmatrix} a_{11} & a_{12} \\ a_{21} & a_{22} \end{bmatrix}, \tag{15}$$

where

$$a_{11} = -X^*\left(b - \frac{Y^*(1-cY^*)^2 a_1}{(X^*(1-cY^*)+K_1)^2} + \frac{eK_2}{(X^*+K_2)^2}\right),$$
$$a_{12} = -X^*\left(\frac{fr}{(1+fY^*)^2} + \frac{cX^*Y^*(1-cY^*)a_1}{(X^*(1-cY^*)+K_1)^2} + \frac{(1-2cY^*)a_1}{X^*(1-cY^*)+K_1}\right),$$

$$a_{21} = \frac{K_1 a_2 (1-cY^*)Y^*}{(X^*(1-cY^*)+K_1)^2} > 0,$$
$$a_{22} = -\frac{K_1 a_2 c X^* Y^*}{(X^*(1-cY^*)+K_1)^2} < 0.$$

The characteristic polynomial of J_{P_3} can be determined as:

$$\lambda^2 - Tr_{P_3}\lambda + Det_{P_3} = 0, \tag{16}$$

where $Tr_{P_3} = a_{11} + a_{22}$, and $Det_{P_3} = a_{11}a_{22} - a_{12}a_{21}$. Clearly, equation (16) has the following roots (eigenvalues):

$$\lambda_{31} = \frac{Tr_{P_3} + \sqrt{(Tr_{P_3})^2 - 4Det_{P_3}}}{2}, \lambda_{32} = \frac{Tr_{P_3} - \sqrt{(Tr_{P_3})^2 - 4Det_{P_3}}}{2}. \tag{17}$$

According to the Routh Hurwitz criterion, the two roots λ_{31} and λ_{32} have negative real parts if and only if $Tr_{P_3} < 0$, and $Det_{P_3} > 0$. Therefore, direct computation shows that the COEP will be LAS if and only if the following sufficient conditions hold.

$$\frac{Y^*(1-cY^*)^2 a_1}{(X^*(1-cY^*)+K_1)^2} \leq b + \frac{eK_2}{(X^*+K_2)^2}. \tag{18}$$

$$Y^* \leq \frac{1}{2c}. \tag{19}$$

However, the COEP becomes:

Unstable point if and only if $Tr_{P_3} > 0$, and $Det_{P_3} > 0$.

Saddle point if and only if $Det_{P_3} < 0$.

Linear centre if and only if $Tr_{P_3} = 0$, and $Det_{P_3} > 0$.

5. Persistence

This section delves into the concept of persistence. Persistence in biology refers to the continued survival of all populations indefinitely whenever they initially exist. Mathematically, system (1) is said to be uniformly persistent if there exists a compact region $U \subseteq int.\mathbb{R}^2_+$ such that every solution $\Phi(T) = (X(T), Y(T))^{\mathrm{T}}$ of system (1) with positive initial condition eventually enters and remains in region U, see [22]. Then the conditions that guarantee the system (1)'s uniform persistence is given in the following theorem

Theorem 3: System (1) is uniformly persistent under the following conditions

$$\left.\begin{array}{l} d_1 < r + a_3 \\ d_2 < \frac{a_2 m}{K_1 + m} \end{array}\right\} \tag{20}$$

Proof: Define the function $\varphi(X,Y) = X^\alpha Y^\beta$, where α and β are positive constants. Clearly $\varphi(X,Y) > 0$ for all $(X,Y) \in int.\mathbb{R}^2_+$ and $\varphi(X,Y) \to 0$ when $X \to 0$ or $Y \to 0$. Furthermore, it's clear that

$$\frac{\varphi'}{\varphi} = \frac{\alpha}{X}\frac{dX}{dT} + \frac{\beta}{Y}\frac{dY}{dT} = \alpha f_1 + \beta f_2,$$

where f_1 and f_2 are given in the system (1). Thus

$$\frac{\varphi'}{\varphi} = \alpha\left[\frac{r}{1+fY} - d_1 - bX + a_3 - \frac{a_1(1-cY)Y}{K_1 + X(1-cY)} - \frac{eX}{K_2+X}\right] + \beta\left[\frac{a_2 X(1-cY)}{K_1 + X(1-cY)} - d_2\right].$$

According to the Lyapunov average method [23], if $\frac{\varphi'}{\varphi} > 0$ for all the boundary equilibrium points, then the solution of system (1) initiates in $int.\mathbb{R}^2_+$ eventually enters and remains in $int.\mathbb{R}^2_+$ for suitable choice of constants $\alpha > 0$ and $\beta > 0$. Now, since

$$\frac{\varphi'}{\varphi}(P_1) = \alpha[r - d_1 + a_3] + \beta[-d_2].$$
$$\frac{\varphi'}{\varphi}(P_2) = \beta\left[\frac{a_2 m}{K_1 + m} - d_2\right].$$

Then the first expression is positive as the positive constants α and β are arbitrary constants and we are always can choose that α is sufficiently larger than β. Hence, the requirements of

the Lyapunov average method are met provided that the conditions (20) hold, which means system (1) is uniformly persistent.

6. Local Bifurcation

This section uses an application of Sotomayor's theorem [24] to identify the potential for local bifurcation. It is well known that the likelihood of local bifurcation is dependent on several conditions, one of which is the existence of a nonhyperbolic equilibrium point type. In the following theorems, the candidate bifurcating parameter is correspondingly chosen to ensure that the analyzed equilibrium point is not a hyperbolic point. Now rewrite system (1) in the vector form as:

$$\frac{d\mathbf{W}}{dT} = \mathbf{F}(\mathbf{W},\mu),\ \mathbf{W} = \begin{pmatrix} X \\ Y \end{pmatrix},\ \mu \in \mathbb{R}_+,\ \mathbf{F}(\mathbf{W},\mu) = \begin{pmatrix} F_1(X,Y,\mu) \\ F_2(X,Y,\mu) \end{pmatrix}. \tag{21}$$

Hence, the second directional derivative of $\mathbf{F}$, where $\mathbf{V} = (v_1, v_2)^{\mathrm{T}}$ be any vector, can be written using direct computation as:

$$D^2\mathbf{F}(\mathbf{W},\mu).(\mathbf{V},\mathbf{V}) = \begin{pmatrix} c_{11} \\ c_{21} \end{pmatrix}, \tag{22}$$

where

$$c_{11} = -\frac{2[b(X+K_2)^3+eK_2^2]v_1^2}{(X+K_2)^3} - \frac{2frv_1v_2}{(1+fY)^2} + \frac{2f^2rXv_2^2}{(1+fY)^3} + \frac{2a_1K_1Y(1-cY)^2v_1^2}{(X(1-cY)+K_1)^3} + \frac{2a_1K_1cX(X+K_1)v_2^2}{(X(1-cY)+K_1)^3} - \frac{2a_1K_1[X(1-cY)+(1-2cY)K_1]v_1v_2}{(X(1-cY)+K_1)^3}.$$

$$c_{21} = -\frac{2a_2K_1Y(1-cY)^2v_1^2}{(X(1-cY)+K_1)^3} + \frac{2a_2K_1[X(1-cY)+(1-2cY)K_1]v_1v_2}{(X(1-cY)+K_1)^3} - \frac{2a_2K_1cX(X+K_1)v_2^2}{(X(1-cY)+K_1)^3}.$$

Theorem 4: When the parameter d_1 crosses through the value $d_1^* = r + a_3$, a transcritical bifurcation (TB) of the system (1) occurs at the VEP.

Proof: From the JM that is written in equation (9), it is observed that, for $d_1 = d_1^*$ it becomes

$$J_1 = J_{P_1,d_1^*} = \begin{bmatrix} 0 & 0 \\ 0 & -d_2 \end{bmatrix}.$$

As a result, J_1's eigenvalues are $\lambda_{11}^* = -d_2$, which is negative, and $\lambda_{11}^* = 0$, which is zero. As a consequence, the VEP fails to be a hyperbolic point. Allow $\mathbf{V}_1 = \begin{pmatrix} v_{11} \\ v_{21} \end{pmatrix}$ and $\mathbf{U}_1 = \begin{pmatrix} u_{11} \\ u_{21} \end{pmatrix}$ to represent the eigenvectors for $\lambda_{11}^* = 0$ and its transpose, respectively. Then, using straightforward mathematical procedures, it is concluded that:

$$\mathbf{V}_1 = \begin{pmatrix} 1 \\ 0 \end{pmatrix},\ \mathbf{U}_1 = \begin{pmatrix} 1 \\ 0 \end{pmatrix}$$

Direct calculation also reveals that:

$$\mathbf{F}_{d_1}(\mathbf{W},d_1) = \begin{pmatrix} -X \\ 0 \end{pmatrix} \Rightarrow \mathbf{F}_{d_1}(P_1,d_1^*) = \begin{pmatrix} 0 \\ 0 \end{pmatrix}.$$

This gives that $\mathbf{U}_1{}^{\mathrm{T}}\mathbf{F}_{d_1}(P_1,d_1^*) = 0$.

$$\mathbf{U}_1{}^{\mathrm{T}}\left[D\mathbf{F}_{d_1}(P_1,d_1^*)\mathbf{V}_1\right] = -1 \neq 0,$$

where $D\mathbf{F}_{d_1}(P_1,d_1^*)$ represents the directional derivative of $\mathbf{F}_{d_1}(\mathbf{W},d_1)$ at (P_1,d_1^*). Additionally, the equation (22) yields the following conclusion.

$$D^2\mathbf{F}(P_1,d_1^*).(\mathbf{V}_1,\mathbf{V}_1) = \begin{pmatrix} -\frac{2(e+bK_2)}{K_2} \\ 0 \end{pmatrix}.$$

Hence, it is simple to verify that $\mathbf{U}_1{}^{\mathrm{T}}[D^2\mathbf{F}(P_1,d_1^*).(\mathbf{V}_1,\mathbf{V}_1)] = -\frac{2(e+bK_2)}{K_2} \neq 0$. Thus, the Sotomayor theorem of local bifurcation [24], specifies that the system (1) possess a TB at the P_1, and that completes the proof.

Therefore, it is easy to confirm that $\mathbf{U}_1{}^{\mathrm{T}}[D^2\mathbf{F}(P_1, d_1^*).(\mathbf{V}_1, \mathbf{V}_1)] = -\frac{2(e+bK_2)}{K_2} \neq 0$. The proof is thus complete because the Sotomayor theorem of local bifurcation states that the system (1) has a TB at the P_1.

Theorem 5: When the parameter a_2 crosses through the value $a_2^* = \frac{(m+K_1)d_2}{m}$, a TB of the system (1) occurs at the AEP.

Proof: From the JM that is written in equation (12), it is observed that, for $a_2 = a_2^*$ it becomes

$$J_2 = J_{P_2,a_2^*} = \begin{bmatrix} -m\left(b + \frac{eK_2}{(m+K_2)^2}\right) & -m\left(f\mathrm{r} + \frac{a_1}{m+K_1}\right) \\ 0 & 0 \end{bmatrix}.$$

As a result, J_2's eigenvalues are $\lambda_{21}^* = -m\left(b + \frac{eK_2}{(m+K_2)^2}\right)$, which is negative, and $\lambda_{22}^* = 0$, which is zero. As a consequence, the AEP fails to be a hyperbolic point. Allow $\mathbf{V}_2 = \begin{pmatrix} v_{12} \\ v_{22} \end{pmatrix}$ and $\mathbf{U}_2 = \begin{pmatrix} u_{12} \\ u_{22} \end{pmatrix}$ to represent the eigenvectors for $\lambda_{22}^* = 0$ and its transpose, respectively. Then, using straightforward mathematical procedures, it is concluded that:

$$\mathbf{V}_2 = \begin{pmatrix} -\frac{[f\mathrm{r}(m+K_1)+a_1](m+K_2)^2}{[\,b(m+K_2)^2+eK_2](m+K_1)} \\ 1 \end{pmatrix} = \begin{pmatrix} \gamma_1 \\ 1 \end{pmatrix}, \mathbf{U}_2 = \begin{pmatrix} 0 \\ 1 \end{pmatrix}.$$

Direct calculation also reveals that:

$$\mathbf{F}_{a_2}(\mathbf{W}, a_2) = \begin{pmatrix} 0 \\ Y\frac{X(1-cY)}{K_1+X(1-cY)} \end{pmatrix} \Rightarrow \mathbf{F}_{a_2}(P_2, a_2^*) = \begin{pmatrix} 0 \\ 0 \end{pmatrix}.$$

This gives that $\mathbf{U}_2{}^{\mathrm{T}}\mathbf{F}_{a_2}(P_2, a_2^*) = 0$.

$$\mathbf{U}_2{}^{\mathrm{T}}\left[D\mathbf{F}_{a_2}(P_2, a_2^*)\mathbf{V}_2\right] = \frac{m}{K_1+m} \neq 0,$$

where $D\mathbf{F}_{a_2}(P_2, a_2^*)$ represents the directional derivative of $\mathbf{F}_{a_2}(\mathbf{W}, a_2)$ at (P_2, a_2^*). Additionally, the equation (22) yields the following conclusion.

$$D^2\mathbf{F}(P_2, a_2^*).(\mathbf{V}_2, \mathbf{V}_2) = \begin{pmatrix} -\frac{2[b(m+K_2)^3+eK_2^2]\gamma_1^2}{(m+K_2)^3} - 2fr\gamma_1 + 2f^2rm + \frac{2a_1K_1cm}{(m+K_1)^2} - \frac{2a_1K_1\gamma_1}{(m+K_1)^2} \\ a_2^*\left(\frac{2K_1\gamma_1}{(m+K_1)^2} - \frac{2K_1cm}{(m+K_1)^2}\right) \end{pmatrix}.$$

Hence, since $\gamma_1 < 0$, it is simple to verify that:

$$\mathbf{U}_2{}^{\mathrm{T}}[D^2\boldsymbol{F}(P_2, a_2^*).(\mathbf{V}_2, \mathbf{V}_2)] = a_2^*\left(\frac{2K_1\gamma_1}{(m+K_1)^2} - \frac{2K_1cm}{(m+K_1)^2}\right) < 0.$$

Thus the Sotomayor theorem of local bifurcation, specifies that the system (1) possess a TB at the P_2, and that completes the proof.

Theorem 6: Assume that condition (19) holds, then the system (1) possesses a saddle-node bifurcation (SNB) at COEP when the parameter b crosses through the value $b^* = \frac{Y^*(1-cY)^2a_1}{(X^*(1-cY)+K_1)^2} - \frac{eK_2}{(X^*+K_2)^2} - \frac{a_{12}a_{21}}{X^*a_{22}}$, if the following requirements are met.

$$\frac{eK_2}{(X^*+K_2)^2} + \frac{a_{12}a_{21}}{X^*a_{22}} < \frac{Y^*(1-cY)^2a_1}{(X^*(1-cY)+K_1)^2}. \quad (23)$$

$$c_{11}(P_3, b^*)\gamma_3 + c_{21}(P_3, b^*) \neq 0. \quad (24)$$

where all the new symbols are given in the proof.

Proof: From the JM that is written in equation (15), it is observed that, for $b = b^*$ it becomes

$$J_3 = J_{P_3,b^*} = \left[a_{ij}^*\right],$$

where $a_{11}^* = a_{11}(b^*)$, $a_{12}^* = a_{12}$, $a_{21}^* = a_{21}$, and $a_{22}^* = a_{22}$. Straightforward computation shows that the determinant of J_3 at $b = b^*$ (i.e. Det_{P_3,b^*}) is zero. Then J_3 has zero eigenvalue

($\lambda_{31}^{*}=0$) with the second eigenvalue $\lambda_{32}^{*}=Tr_{P_3,b^*}$. Thus, the COEP is a non-hyperbolic point when $b=b^*$.

Allow $\mathbf{V}_3=\begin{pmatrix}v_{13}\\v_{23}\end{pmatrix}$ and $\mathbf{U}_3=\begin{pmatrix}u_{13}\\u_{23}\end{pmatrix}$ to represent the eigenvectors for $\lambda_{31}^{*}=0$ and its transpose, respectively. Then, using straightforward mathematical procedures, it is concluded that:

$$\mathbf{V}_3=\begin{pmatrix}-\frac{a_{12}}{a_{11}^{*}}\\1\end{pmatrix}=\begin{pmatrix}\gamma_2\\1\end{pmatrix},\ \mathbf{U}_3=\begin{pmatrix}-\frac{a_{21}}{a_{11}^{*}}\\1\end{pmatrix}=\begin{pmatrix}\gamma_3\\1\end{pmatrix}.$$

According to the elements of J_3 and the condition (23), it is observed that $\gamma_2>0$, and $\gamma_3<0$. Direct calculation also reveals that

$$\mathbf{F}_b(\mathbf{W},b)=\begin{pmatrix}-X^2\\0\end{pmatrix}\Rightarrow \mathbf{F}_b(P_3,b^*)=\begin{pmatrix}-X^{*2}\\0\end{pmatrix}.$$

This gives that $\mathbf{U}_3{}^{\mathrm{T}}\mathrm{F}_b(P_3,b^*)=-\gamma_3X^{*2}>0$. Moreover, from the equation (22), the following finding is obtained

$$D^2\mathbf{F}(P_3,b^*).(\mathbf{V}_3,\mathbf{V}_3)=\begin{pmatrix}c_{11}(P_3,b^*)\\c_{21}(P_3,b^*)\end{pmatrix},$$

where

$$c_{11}(P_3,b^*)=-\frac{2[b^*(X^*+K_2)^3+eK_2^2]\gamma_2^2}{(X^*+K_2)^3}-\frac{2fr\gamma_2}{(1+fY^*)^2}+\frac{2f^2rX^*}{(1+fY^*)^3}+\frac{2a_1K_1Y^*(1-cY^*)^2\gamma_2^2}{(X^*(1-cY^*)+K_1)^3}+\frac{2a_1K_1cX^*(X^*+K_1)}{(X^*(1-cY^*)+K_1)^3}-\frac{2a_1K_1[X^*(1-cY^*)+(1-2cY^*)K_1]\gamma_2}{(X^*(1-cY^*)+K_1)^3}.$$

$$c_{21}(P_3,b^*)=-\frac{2a_2K_1Y^*(1-cY^*)^2\gamma_2^2}{(X^*(1-cY^*)+K_1)^3}+\frac{2a_2K_1[X^*(1-cY^*)+(1-2cY^*)K_1]\gamma_2}{(X^*(1-cY^*)+K_1)^3}-\frac{2a_2K_1cX^*(X^*+K_1)}{(X^*(1-cY^*)+K_1)^3}.$$

Therefore, it is easy to confirm that using the condition (24).

$$\mathbf{U}_3{}^{\mathrm{T}}[D^2\mathbf{F}(P_3,b^*).(\mathbf{V}_3,\mathbf{V}_3)]=c_{11}(P_3,b^*)\gamma_3+c_{21}(P_3,b^*)\neq 0.$$

The proof is thus complete because the Sotomayor theorem of local bifurcation states that the system (1) has an SNB at the P_3.

7. Global stability

Here, we provide the result to attain global asymptotic stability (GAS) for each equilibrium point of the system (1).

Theorem 7: The VEP is globally asymptotically stable whenever it is LAS.

Proof: Consider the scalar function $V_1=X+Y$.

Obviously, $V_1:\mathbb{R}_+^2\to\mathbb{R}$, such that $V_1(P_1)=0$ and $V_1(u,v)>0$, $\forall\ (u,v)\neq P_1$ with $(u,v)\in\mathbb{R}_+^2$.

Accordingly, V_1 is a positive definite function. The derivative of V_1 can be determined as

$$\frac{dV_1}{dT}=\frac{dX}{dT}+\frac{dY}{dT}<(r+a_3-d_1)X-d_2Y.$$

Therefore, due to local stability condition (11), it is obtained that $\frac{dV_1}{dT}<0$ and $\frac{dV_1}{dT}=0$ only at P_1 that means $\frac{dV_1}{dT}$ is a negative definite function. Moreover, since $V_1(\boldsymbol{W})\to\infty$ whever $\|\boldsymbol{W}\|\to\infty$ with $\boldsymbol{W}=\begin{pmatrix}X\\Y\end{pmatrix}$, then it is a radial unbounded function. Therefore, according to the global stability theorem [25], the VEP is a GAS.

Theorem 8: The AEP is a GAS provided that

$$m(rf+a_1)<d_2. \tag{25}$$

Proof: Consider the scalar function $V_2=\left(X-m-m\ln\left(\frac{X}{m}\right)\right)+Y$.

Obviously, $V_2:\mathbb{R}_+^2\to\mathbb{R}$, such that $V_2(P_2)=0$ and $V_2(u,v)>0$, $\forall\ (u,v)\neq P_2$ with $(u,v)\in\mathbb{R}_+^2$.

Accordingly, V_2 is a positive definite function. The derivative of V_2 can be determined as

$$\frac{dV_2}{dT} = \frac{(X-m)}{X}\frac{dX}{dT} + \frac{dY}{dT} = (X-m)\left[-r\frac{fY}{1+fY} - b(X-m) - \frac{a_1(1-cY)Y}{K_1+X(1-cY)} - e\left(\frac{K_2(X-m)}{(K_2+X)(K_2+m)}\right)\right] + \frac{a_2X(1-cY)Y}{K_1+X(1-cY)} - d_2Y.$$

Therefore

$$\frac{dV_2}{dT} \leq -\left[b + e\left(\frac{K_2}{(K_2+X)(K_2+m)}\right)\right](X-m)^2 - \frac{rfXY}{1+fY} + \frac{rfmY}{1+fY} + \frac{a_1m(1-cY)Y}{K_1+X(1-cY)} - d_2Y$$

$$< -\left[b + e\left(\frac{K_2}{(K_2+X)(K_2+m)}\right)\right](X-m)^2 - [d_2 - m(rf+a_1)]Y$$

Therefore, due to condition (25), it is obtained that $\frac{dV_2}{dT} < 0$ and $\frac{dV_2}{dT} = 0$ only at P_2 that means $\frac{dV_2}{dT}$ is a negative definite function. Moreover, since $V_2(\mathbf{W}) \to \infty$ whever $\|\mathbf{W}\| \to \infty$ with $\mathbf{W} = \begin{pmatrix} X \\ Y \end{pmatrix}$, then it is a radial unbounded function. Therefore, according to the global stability theorem, the AEP is a GAS.

Theorem 9: The COEP is a GAS provided that the following conditions are met.

$$\frac{a_1[(1-cY)(1-cY^*)Y^*]}{\Lambda_3\Lambda_3^*} < \frac{rf}{\Lambda_1\Lambda_1^*} + b + \frac{eK_2}{\Lambda_2\Lambda_2^*}. \quad (26)$$

$$\rho_{12}{}^2 < 4\rho_{11}\rho_{22}. \quad (27)$$

where all the new symbols are given in the proof.

Proof: Consider the scalar function $V_3 = \left(X - X^* - X^*\ln\left(\frac{X}{X^*}\right)\right) + \left(Y - Y^* - Y^*\ln\left(\frac{Y}{Y^*}\right)\right)$. Obviously, $V_3: \mathbb{R}_+^2 \to \mathbb{R}$, such that $V_3(P_3) = 0$ and $V_3(u,v) > 0$, $\forall\ (u,v) \neq P_3$ with $(u,v) \in \mathbb{R}_+^2$.

Accordingly, V_3 is a positive definite function. The derivative of V_3 can be determined as

$$\frac{dV_3}{dT} = \frac{(X-X^*)}{X}\frac{dX}{dT} + \frac{(Y-Y^*)}{Y}\frac{dY}{dT} = -\frac{rf}{\Lambda_1\Lambda_1^*}(X-X^*)^2 - b(X-X^*)^2 + \frac{a_1[(1-cY)(1-cY^*)Y^*]}{\Lambda_3\Lambda_3^*}(X-X^*)^2 - \frac{eK_2}{\Lambda_2\Lambda_2^*}(X-X^*)^2 - \frac{a_1[\Lambda_2^* - c\Lambda_2^*(Y+Y^*) + X^*Y^*Y]}{\Lambda_3\Lambda_3^*}(X-X^*)(Y-Y^*) + \frac{a_2K_1(1-cY)}{\Lambda_3\Lambda_3^*}(X-X^*)(Y-Y^*) - \frac{a_2cX^*(K_1+X^*)}{\Lambda_3\Lambda_3^*}(Y-Y^*)^2$$

where

$$\Lambda_1 = (1+fY), \Lambda_1^* = (1+fY^*), \Lambda_2 = (K_2+X), \Lambda_2^* = (K_2+X^*).$$
$$\Lambda_3 = [K_1 + X(1-cY)], \Lambda_3^* = [K_1 + X^*(1-cY^*)].$$

Therefore, it is obtained that

$$\frac{dV_3}{dT} = -\left[\frac{rf}{\Lambda_1\Lambda_1^*} + b - \frac{a_1[(1-cY)(1-cY^*)Y^*]}{\Lambda_3\Lambda_3^*} + \frac{eK_2}{\Lambda_2\Lambda_2^*}\right](X-X^*)^2 - \frac{a_2cX^*(K_1+X^*)}{\Lambda_3\Lambda_3^*}(Y-Y^*)^2 - \left[\frac{a_1[\Lambda_2^* - c\Lambda_2^*(Y+Y^*) + X^*Y^*Y] - a_2K_1(1-cY)}{\Lambda_3\Lambda_3^*}\right](X-X^*)(Y-Y^*)$$

$$= -[\rho_{11}(X-X^*)^2 + \rho_{12}(X-X^*)(Y-Y^*) + \rho_{22}(Y-Y^*)^2]$$

Now, using the conditions (26)-(27), it is obtained that

$$\frac{dV_3}{dT} < -\left[\sqrt{\rho_{11}}(X-X^*) + \sqrt{\rho_{22}}(Y-y^*)\right]^2$$

Obviously, $\frac{dV_3}{dT}$ is a negative definite function, which is $\frac{dV_3}{dT} = 0$ only at P_3. Moreover, since $V_3(\mathbf{W}) \to \infty$ whenever $\|\mathbf{W}\| \to \infty$ with $\mathbf{W} = \begin{pmatrix} X \\ Y \end{pmatrix}$, then it is a radial unbounded function. Therefore, according to the global stability theorem, the COEP is a globally asymptotically stable.

8. Hopf bifurcation

The Hopf bifurcation occurrence at the COEP is analyzed by selecting a_1 as the bifurcation parameter. According to the JM at P_3 given in equation (15), the characteristic equation was determined in equation (16) depending on JM's trace $\left(Tr_{P_3} = a_{11} + a_{22}\right)$ and determinant $\left(Det_{P_3} = a_{11}a_{22} - a_{12}a_{21}\right)$, where $a_{ij}, i, j = 1,2$ are the JM elements. Therefore, the following theorem provides the necessary and sufficient condition for having a Hopf bifurcation.

Theorem 10. When the parameter a_1 passes through a_1^*, the system (1) undergoes a Hopf bifurcation around COEP provided that the following condition is met.

$$cX^*\left(b + \frac{eK_2}{(X^*+K_2)^2}\right) + \left(\frac{fr(1-cY^*)}{(1+fY^*)^2} + \frac{(1-cY^*)(1-2cY^*)a_1^*}{X^*(1-cY^*)+K_1}\right) > 0, \tag{28}$$

where

$$a_1^* = \frac{K_1 a_2 cY^*}{Y^*(1-cY^*)^2} + \frac{(X^*(1-cY^*)+K_1)^2}{Y^*(1-cY^*)^2}\left[b + \frac{eK_2}{(X^*+K_2)^2}\right].$$

Proof. At $a_1 = a_1^*$, the $Tr_{P_3} = a_{11} + a_{22} = 0$, and hence the characteristic equation (16) becomes

$$\lambda^2 + Det_{P_3} = 0. \tag{29}$$

Moreover, since $Det_{P_3} = a_{11}a_{22} - a_{12}a_{21}$, hence $Det_{P_3}(a_1^*) > 0$ under the condition (28).

Clearly, the equation (29) has roots $\lambda_1 = i\sqrt{Det_{P_3}(a_1^*)}$ and $\lambda_2 = -i\sqrt{Det_{P_3}(a_1^*)}$. Thus JM of the system (1) has two purely imaginary eigenvalues at (P_3, a_1^*).

Note that, Tr_{P_3} and Det_{P_3} are smooth functions of a_1. Therefore, in the neighbourhood of a_1, the characteristic equation (16)'s roots are written in the form

$$\lambda_1 = \sigma_1(a_1) + i\sigma_2(a_1) = \frac{Tr_{P_3} + \sqrt{\left(Tr_{P_3}\right)^2 - 4Det_{P_3}}}{2},$$

$$\lambda_2 = \sigma_1(a_1) - i\sigma_2(a_1) = \frac{Tr_{P_3} - \sqrt{\left(Tr_{P_3}\right)^2 - 4Det_{P_3}}}{2},$$

where $\sigma_i(a_1); i = 1,2$ are real functions.

Now, due to Hopf bifurcation theorem [1], the proof follows if the transversality condition $\frac{d}{da_1} Re\ \lambda_i(a_1)|_{a_1=a_1^*} \neq 0$ is satisfied.

Since $Re\ \lambda_i(a_1) = \sigma_1(a_1) = \frac{Tr_{P_3}}{2}$, then direct computation gives that:

$$\frac{d}{da_1} Re\ \lambda_i(a_1) = \frac{d}{da_1}\sigma_1(a_1) = \frac{X^*Y^*(1-cY^*)^2}{(X^*(1-cY^*)+K_1)^2}.$$

Accordingly, $\frac{d}{da_1} Re\ \lambda_i(a_1)|_{a_1=a_1^*} = \frac{X^*Y^*(1-cY^*)^2}{(X^*(1-cY^*)+K_1)^2} \neq 0$.

Hence, the system (1) undergoes a Hopf bifurcation at P_3 when $a_1 = a_1^*$.

9. Numerical simulation

In this section, a few numerical simulations were run using MATLAB code for solving and drawing the phase portrait and Mathematica of version 12 for the preparing the direction field to test our analytical conclusions and investigate the impact of parameters on the dynamical behavior of the system (1). Accordingly, System (1) with the following hypothetical fixed parameters Dataset is investigated.

$$\begin{aligned} &r = 2, f = 0.2, b = 0.2, d_1 = 0.1, a_1 = 0.5, c = 0.4 \\ &K_1 = 1, a_2 = 0.25, a_3 = 0.1, e = 0.4, K_2 = 1, d_2 = 0.15 \end{aligned}. \tag{30}$$

It is observed that for the dataset (30), system (1) has a unique COEP given by $P_3 = (5.18, 1.77)$ which is an asymptotic stable point and two boundary saddle points $P_1 = (0, 0)$ and $P_2 = (8.21, 0)$ as shown in figure 1. In the following figures, the red and black points represent the equilibrium points and initial points respectively, while the black arrows represent the direction of the trajectories.

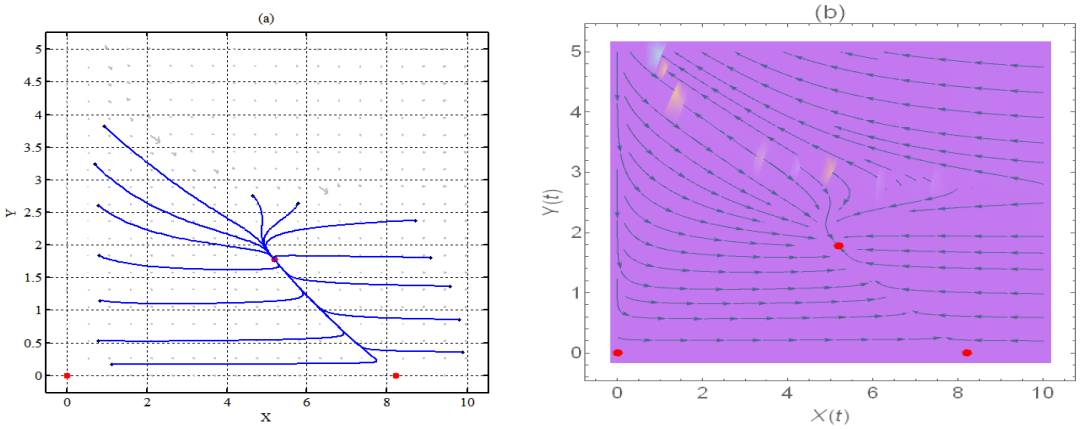

Figure 1: *For Dataset (30), the system (1)'s (a) Phase portrait. (b) Existence of equilibrium points and direction field.*

According to Figure 1, it is clear that the trajectories from different initial points approach asymptotically to the unique COEP. Moreover, a direction field is a mathematical object that graphically represents solutions to a first-order differential equation so that a line segment appears at each point with a slope equal to the slope of a solution to the differential equation passing through the corresponding point given in the phase portrait.

The influence of varying the parameters on the system (1)'s dynamical behavior is investigated numerically. The obtained results are drawn in the form of phase portraits and direction fields. For the parameter r, it is observed that for the range $r \in (0,0.55)$ the COEP disappears and the AEP becomes an asymptotic stable point, see Figure 2 at a selected value.

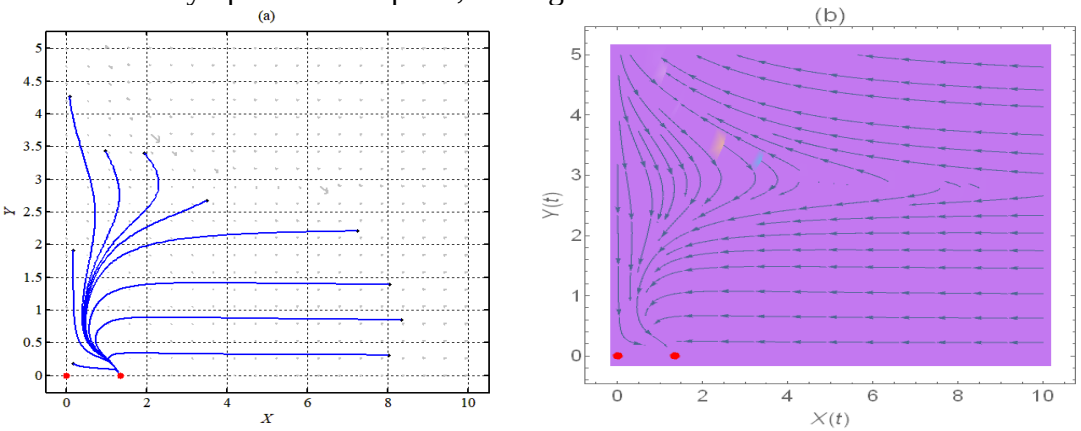

Figure 2: *For Dataset (30) with* $r = 0.5$*, the system (1)'s (a) Phase portrait approaches to* $P_2 = (1.35, 0)$*. (b) Existence of equilibrium points and direction field.*

The effect of varying the parameter f is investigated in Figure 3.

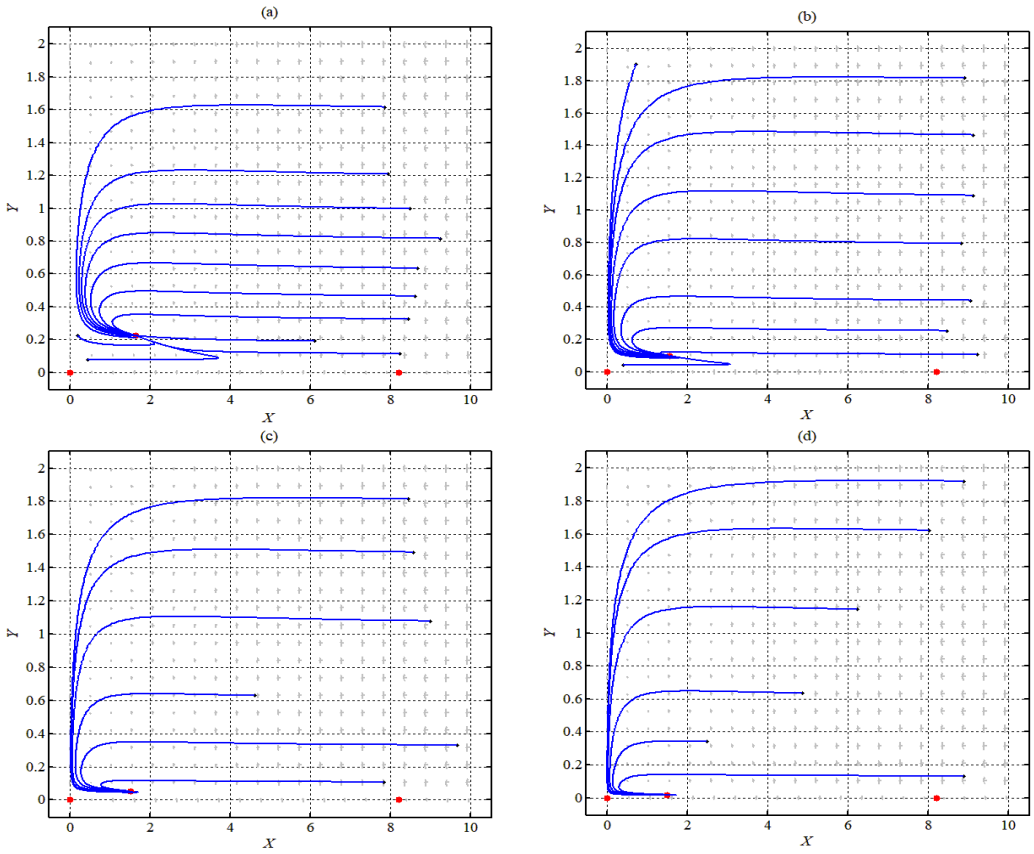

Figure 3: *For Dataset (30) with different values of f, the system (1)'s (a) Phase portrait for $f = 10$ approaches to $P_3 = (1.64, 0.22)$. (b) Phase portrait for $f = 25$ approaches to $P_3 = (1.56, 0.09)$. (c) Phase portrait for $f = 50$ approaches to $P_3 = (1.53, 0.05)$. (d) Phase portrait for $f = 150$ approaches to $P_3 = (1.51, 0.01)$.*

According to Figure (3), although system (1) approaches COEP for different values of f, the predator population decreases approaching zero as the value of f increases.

The effect of changing the parameter b on the dynamics of the system (1) was investigated using the data set (30) with different values of b and the obtained results were presented in Figure 4. It is evident from Figure 4 that the asymptotically stable COEP gradually approaches the AEP, and coincides with each other at $b = 1.18$.

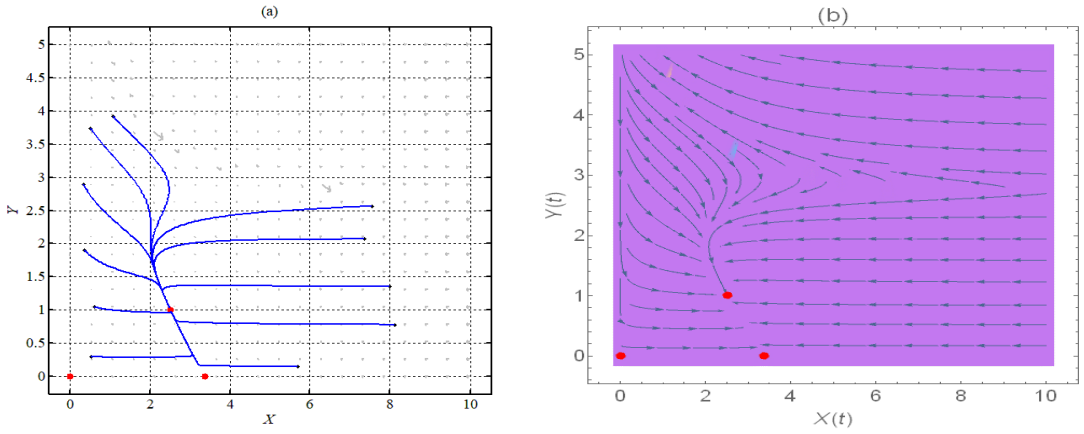

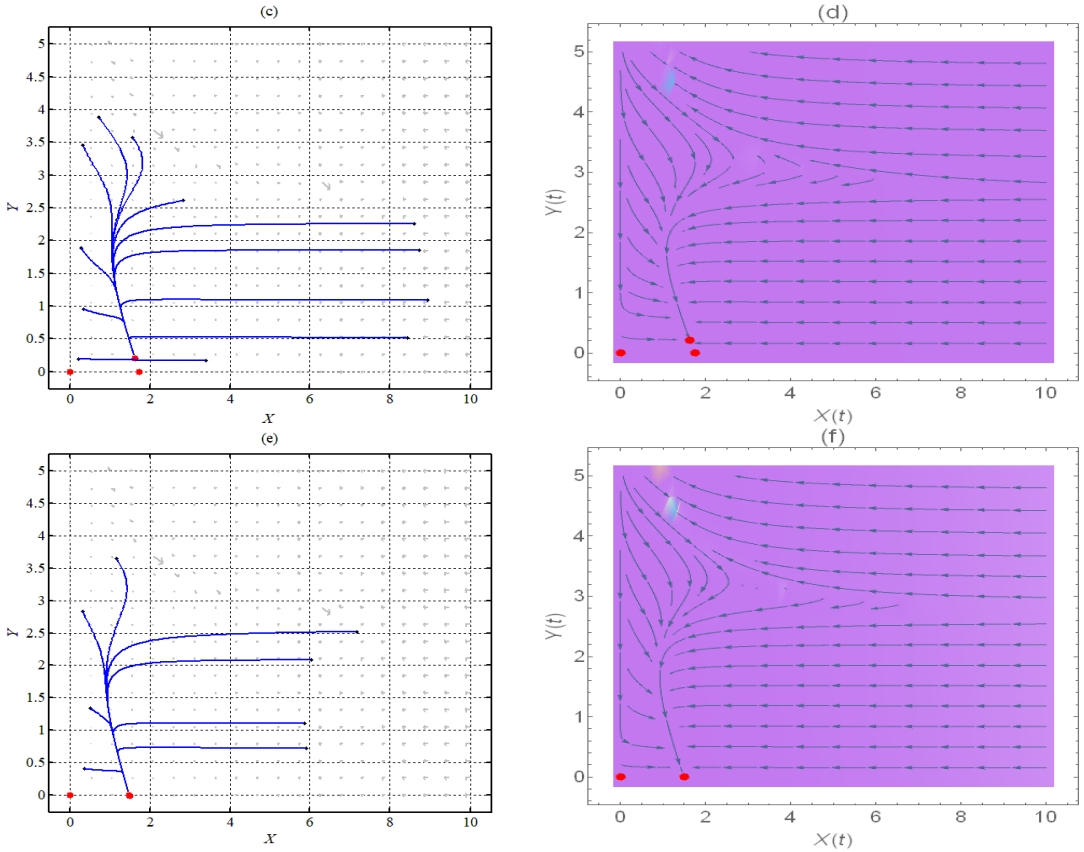

Figure 4: *For Dataset (30) with different values of b, the system (1)'s (a) Phase portrait for* $b = 0.5$ *approaches to* $P_3 = (2.51, 1)$. *(b) Existence of equilibrium points and direction field for* $b = 0.5$. *(c) Phase portrait for* $b = 1$ *approaches to* $P_3 = (1.63, 0.2)$. *(d) Existence of equilibrium points and direction field for* $b = 1$. *(e) Phase portrait for* $b = 1.18$ *approaches to* $P_2 = (1.49,0)$. *(f) Existence of equilibrium points and direction field for* $b = 1.18$.

Figure 5 investigates the influence of varying the parameter a_1 on the dynamic behavior of the system (1). It is observed that the behavior of the trajectories of system (1) near the COEP with increasing the value of a_1 transfers from nodal sink to spiral sink, then becomes unstable at $a_1 = 4.24$ and a Hopf bifurcation occurs. However the boundary points are saddle points.

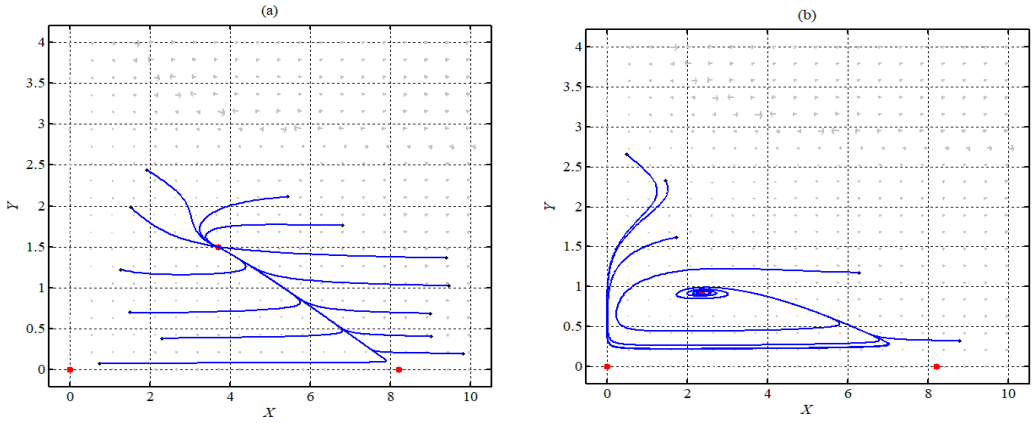

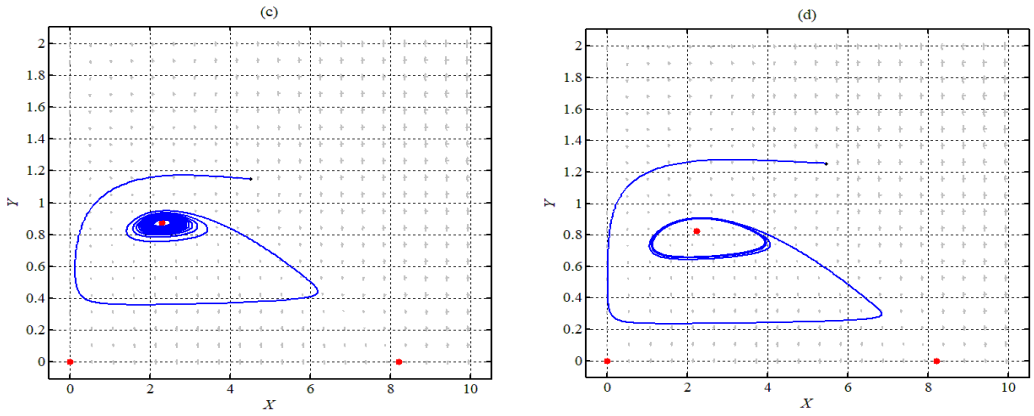

Figure 5: *For Dataset (30) with different values of* a_1 *, the system (1)'s (a) Phase portrait for* $a_1 = 2$ *approaches to nodal sink* $P_3 = (3.71, 1.49)$*. (b) Phase portrait for* $a_1 = 4$ *approaches to spiral sink* $P_3 = (2.37, 0.92)$*. (c) Trajectory approaches to small limit cycle around the source point* $P_3 = (2.3, 0.87)$ *for* $a_1 = 4.24$*. (d) Trajectory approaches to bigger limit cycle around the source point* $P_3 = (2.23, 0.82)$ *for* $a_1 = 4.5$*.*

Clearly, Figure 5 ensures the obtained theoretical results regarding the Hopf bifurcation. The influence of varying c on the dynamic of system (1) is investigated Figure 6.

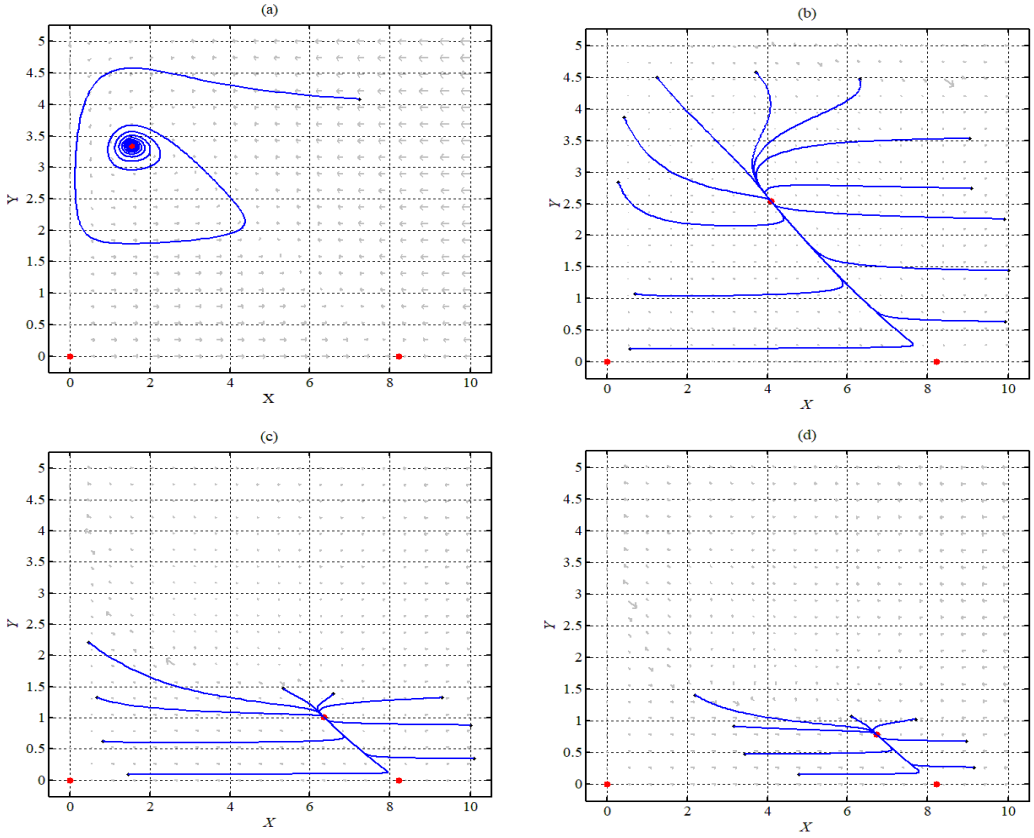

Figure 6: *For Dataset (30) with different values of c, the system (1)'s (a) Trajectory approaches to a spiral sink* $P_3 = (1.55, 3.33)$ *for* $c = 0.01$*. (b) Phase portrait for* $c = 0.25$ *approaches to a nodal sink* $P_3 = (4.09, 2.53)$*. (c) Phase portrait for* $c = 0.75$ *approaches to a nodal sink* $P_3 = (6.34, 1.01)$*. (d) Phase portrait for* $c = 0.99$ *approaches to a nodal sink* $P_3 = (6.72, 0.78)$*.*

The influence of varying the parameter K_1 on the system (1)'s dynamic is explained in Figure 7. It is observed that for the range $K_1 \in (0.01, 0.09)$ there are three COEPs, source, saddle, and nodal sink while the boundary equilibrium points are saddle points. While increasing the value of this parameter gradually makes the COEP approaches AEP, they coincide with each other at $K_1 = 5.48$.

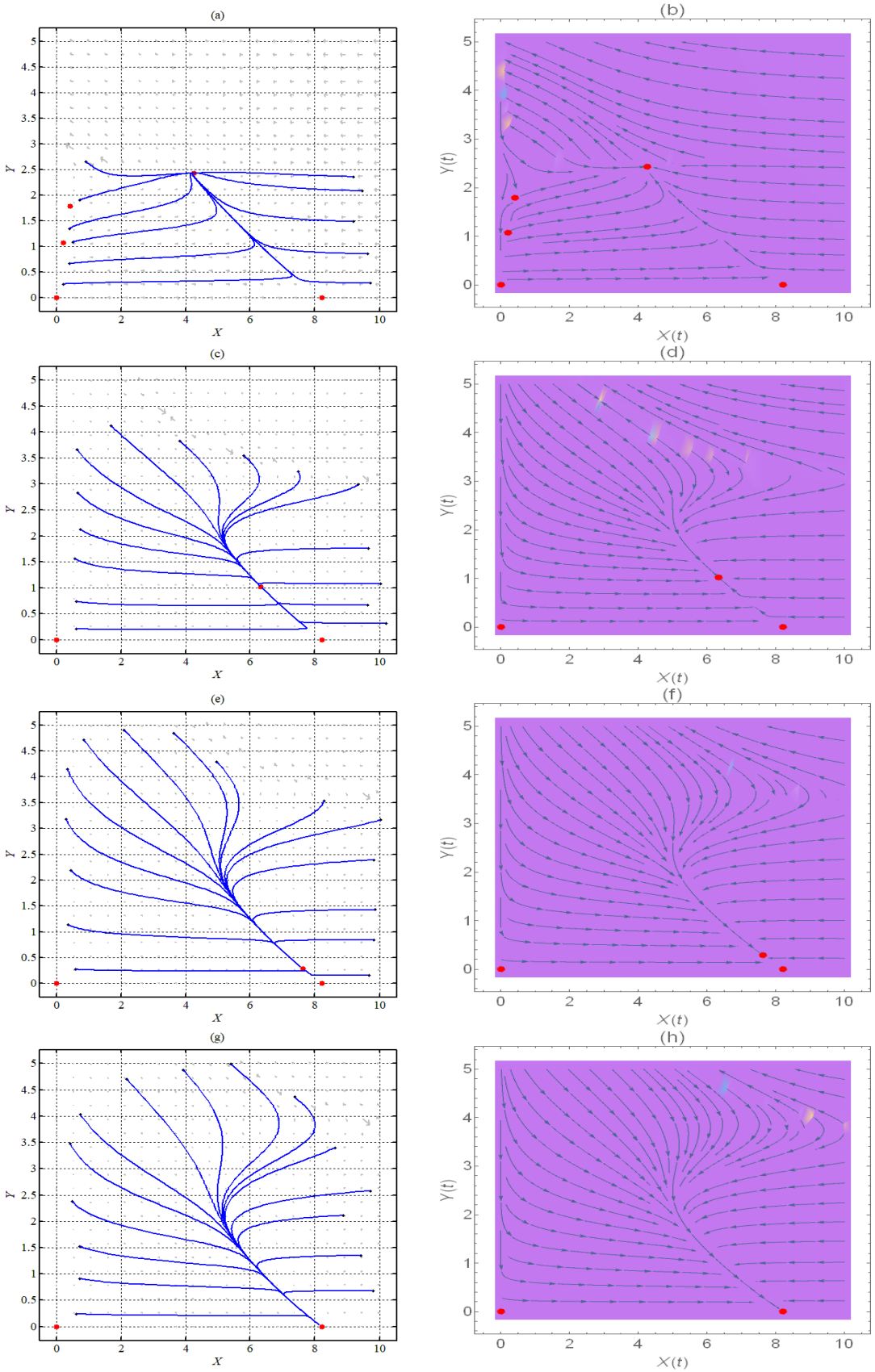

Figure 7: *For Dataset (30) with different values of* K_1*, the system (1)'s (a) Phase portrait for* $K_1 = 0.08$ *approaches to a nodal sink* $P_3 = (4.25, 2.42)$*. (c) Phase portrait for* $K_1 = 2.5$ *approaches to a nodal sink* $P_3 = (6.33, 1.02)$*. (e) Phase portrait for* $K_1 = 4.5$ *approaches to a nodal sink* $P_3 = (7.62, 0.28)$*. (g) Phase portrait for* $K_1 = 5.5$ *approaches to a nodal sink* $P_2 = (8.21, 0)$*. (b), (d), (f), and (h) are the direction fields for* $K_1 = 0.08, 2.5, 4.5,$ *and* 5.5 *respectively.*

Figure 8 demonstrates the influence of varying the parameter a_2 on the dynamic of the system (1). It is noted that for the range $a_2 \in (0,0.16)$ the COEP does not exists and the AEP is nodal sink. Otherwise, the system (1) approaches asymptotically to COEP.

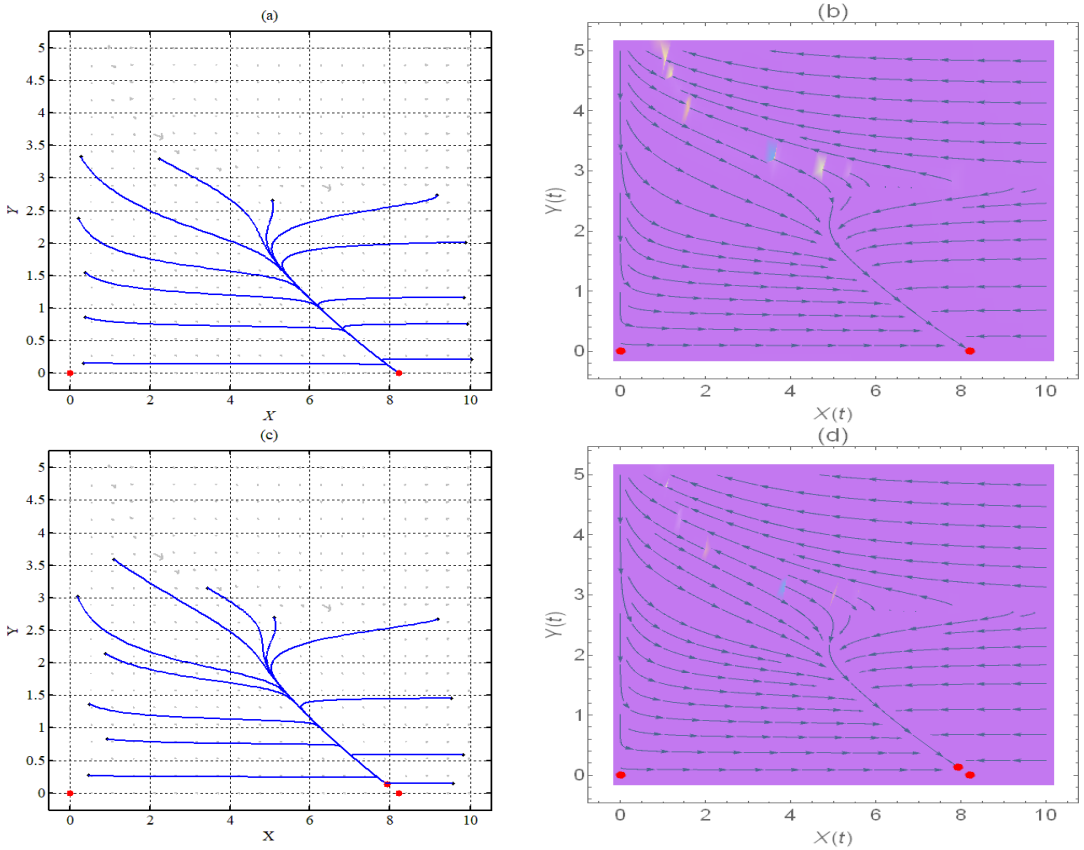

Figure 8: *For Dataset (30) with different values of a_2, the system (1)'s (a) Phase portrait for $a_2 = 0.15$ approaches to $P_2 = (8.21, 0)$. (b) Existence of equilibrium points and direction field for $a_2 = 0.15$. (c) Phase portrait for $a_2 = 0.17$ approaches to $P_3 = (7.92, 0.13)$. (d) Existence of equilibrium points and direction field for $a_2 = 0.17$.*

The influence of the parameter a_3 on the dynamic of the system (1) is studied numerically. It is noted that system (1) still approaches COEP asymptotically with quantitative change in the population size. However, decreasing a_3 together with r so that the prey's survival condition is reflected makes the system (1) approaches asymptotically to the VEP as shown in Figure 9.

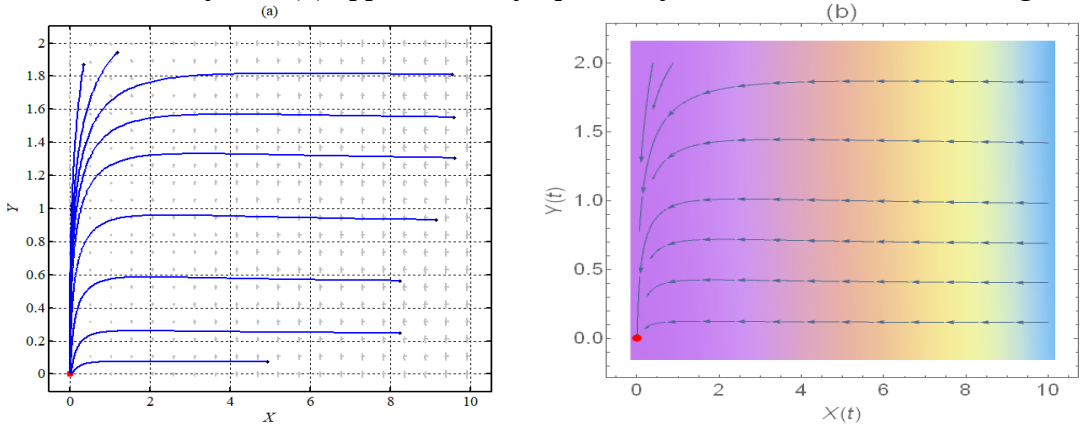

Figure 9: *For Dataset (30), the system (1)'s (a) Phase portrait for $a_3 = 0.01$ and $r = 0.08$ approaches nodal sink $P_1 = (0,0)$. (b) Existence of equilibrium points and direction field.*

The influence of the parameter e on the dynamic of system (1) is investigated in the Figure 10. It is clear from the Figure 10 that as e increases the COEP approaches gradually to AEP, they are coincide with each other at $e = 2.84$.

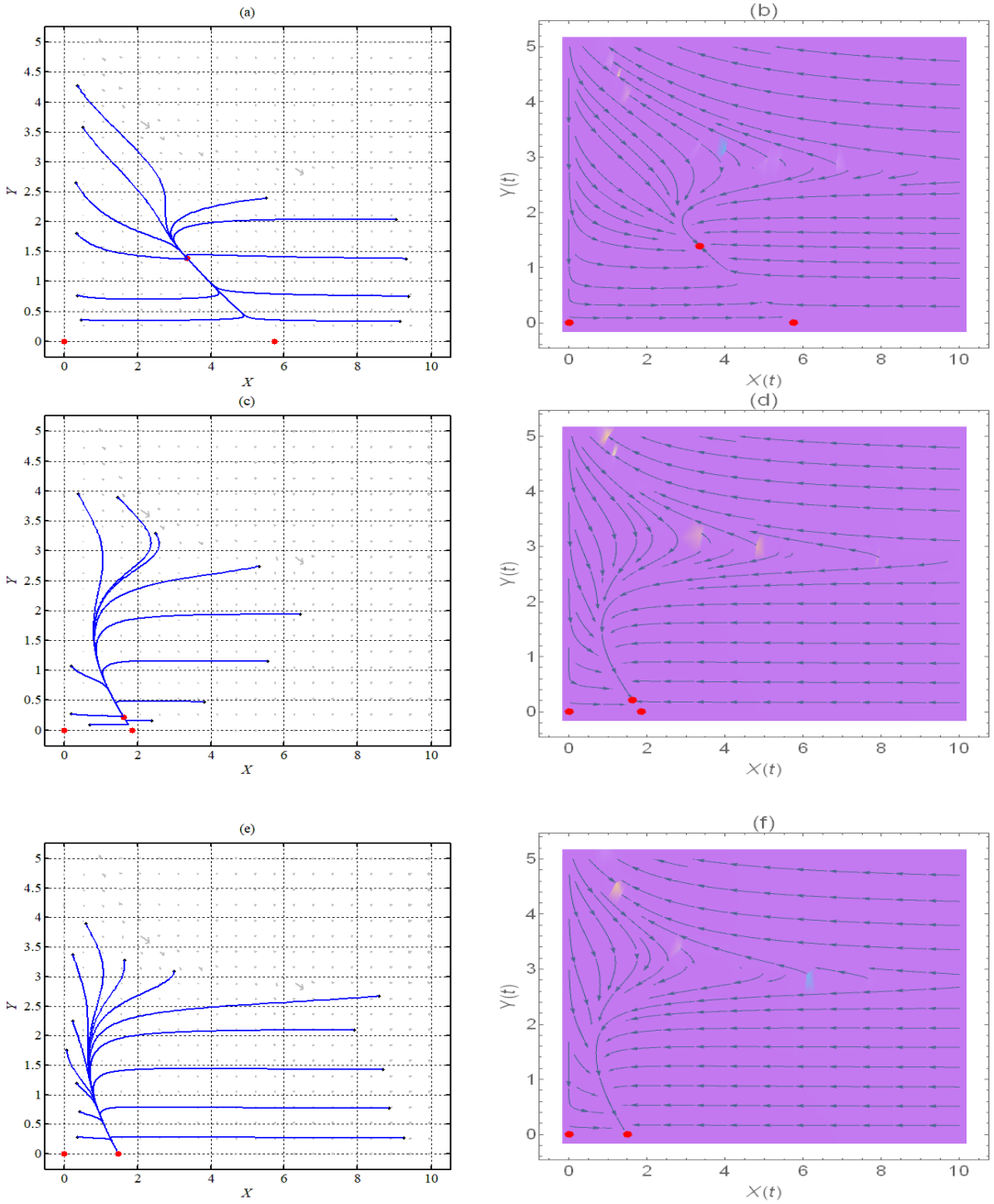

Figure 10: *For Dataset (30) with different values of e, the system (1)'s (a) Phase portrait for* $e = 1$ *approaches to a nodal sink* $P_3 = (3.36, 1.38)$. *(c) Phase portrait for* $e = 2.5$ *approaches to a nodal sink* $P_3 = (1.63, 0.21)$. *(e) Phase portrait for* $e = 2.84$ *approaches to a nodal sink* $P_2 = (1.49, 0)$. *(b), (d), and (f) are the direction fields for* $e = 1, 2.5,$ *and* 2.84 *respectively.*

Finally, Figure 11 demonstrates the influence of d_2 on the dynamic of the system (1). It is noted that as $d_2 \geq 0.24$ the COEP disappears and the system (1) approaches asymptotically AEP.

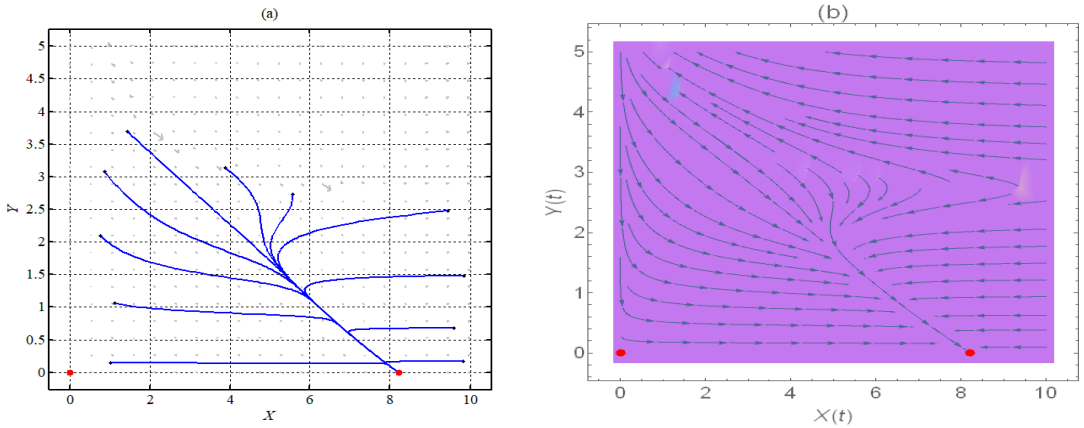

Figure 11: For Dataset (30), the system (1)'s (a) Phase portrait for $d_2 = 0.24$ approaches nodal sink $P_2 = (8.21,0)$. (b) Existence of equilibrium points and direction field for $d_2 = 0.24$.

Finally, the influence of the parameter f on the existence of limit cycle that shown in figure 5d is studied and the obtained result is presented in Figure 12. It is noted that the increase of the value of f lead to stabilize the system (1).

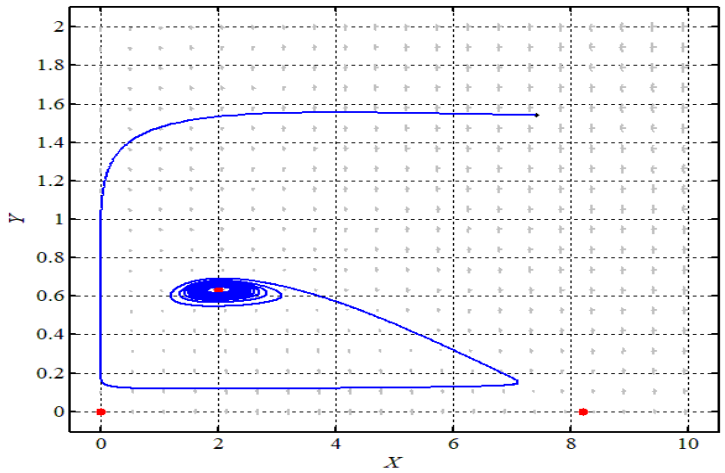

Figure 12: *For Dataset (30), with* $a_1 = 4.5$ *and* $f = 0.5$ *the system (1)'s Phase portrait approaches spiral sink* $P_3 = (2, 0.63)$.

10. Conclusions

In this paper, the prey-predator model involving cannibalism and predator-dependent refuge in the prey population had been proposed and studied. All the properties of the solution were investigated. All possible equilibrium points were determined by their existence conditions. The local stability analysis of the model had been studied. It was obtained that all the equilibrium points are conditionally locally stable. The persistence requirements were obtained. It was proved that system (1) undergoes a TB near the boundary equilibrium points, while an SNB was detected near the COEP. The global dynamics of the system (1) were studied with the help of the Lyapunov function. Finally, the system was investigated numerically to confirm the theoretical findings and detect the parameters' influence on the system (1)'s dynamic behavior. The numerical simulation results are summarized as follows.

For Dataset (30), system (1) has two saddle boundary equilibrium points and asymptotic stale COEP. Decreasing the prey's birth rate or the conversion rate of prey biomass into predator birth below a specific value leads to extinction in the predator population and the system (1) approaches AEP asymptotically. Rising the prey's fear level has a stabilizing effect on the

dynamic behavior of the system up to vital value then the system loses its persistence and approaches to AEP. When prey intraspecific competition rises above a certain threshold, the predator population goes extinct and system (1) gets closer to AEP. Regarding increases in the value of the prey's natural death rate or predator's natural death rate or cannibalism rate in prey, a similar influence on the system's dynamic behavior (1) had been registered as observed in the case of the prey's intraspecific competition. On the other hand, the rise in the prey's refuge rate causes an increase in prey population and a decrease in the predator population but the system (1) still approaches COEP. While decreasing the half-saturation constant of the prey results in the existence of multiple COEPs, however, raising this value above the critical value causes extinction in the predator population and the system (1) approaches AEP. Finally, decreasing the conversion rate of cannibalism into prey birth and the prey's birth rate simultaneously causes extinction in both populations and the system (1) approaches VEP.

References

[1] J. D. Murray, "*Mathematical biology. I: An Introduction,"3rd Edition, Springer-Verlag Berlin Heidelberg*, 2002.

[2] V. H. W. Rudolf, "The impact of cannibalism in the prey on predator–prey systems," *Ecology*, vol. 89, no. 11, pp. 3116–3127, Nov. 2008, doi: 10.1890/08-0104.1.

[3] K. Takatsu, "Predator cannibalism can shift prey community composition toward dominance by small prey species," *Ecol Evol*, vol. 12, no. 5, p. e8894, May 2022, doi: 10.1002/ECE3.8894.

[4] H. Deng, F. Chen, Z. Zhu, and Z. Li, "Dynamic behaviors of Lotka–Volterra predator–prey model incorporating predator cannibalism," *Adv Differ Equ*, vol. 2019, no. 1, pp. 1–17, Dec. 2019, doi: 10.1186/S13662-019-2289-8/FIGURES/10.

[5] F. Zhang, Y. Chen, and J. Li, "Dynamical analysis of a stage-structured predator-prey model with cannibalism," *Math Biosci*, vol. 307, pp. 33–41, Jan. 2019, doi: 10.1016/J.MBS.2018.11.004.

[6] M. Rayungsari, A. Suryanto, W. M. Kusumawinahyu, and I. Darti, "Dynamical Analysis of a Predator-Prey Model Incorporating Predator Cannibalism and Refuge," *Axioms*, vol. 11, no. 3, p. 116, Mar. 2022, doi: 10.3390/AXIOMS11030116.

[7] A. S. Abdulghafour and R. K. Naji, "Modeling and analysis of a prey-predator system incorporating fear, predator-dependent refuge, and cannibalism," *Communications in Mathematical Biology and Neuroscience*, vol. 2022, 2022, doi: 10.28919/cmbn/7722.

[8] Z. Ma, W. Li, Y. Zhao, W. Wang, H. Zhang, and Z. Li, "Effects of prey refuges on a predator-prey model with a class of functional responses: The role of refuges," *Math Biosci*, vol. 218, no. 2, pp. 73–79, Apr. 2009, doi: 10.1016/J.MBS.2008.12.008.

[9] B. Sahoo and S. Poria, "Effects of additional food in a delayed predator-prey model," *Math Biosci*, vol. 261, pp. 62–73, Mar. 2015, doi: 10.1016/J.MBS.2014.12.002.

[10] B. Sahoo, "Dynamical Behaviour of an Epidemic Model with Disease in Top-Predator Population Only: A Bifurcation Study," *Differential Equations and Dynamical Systems*, vol. 28, no. 1, pp. 153–176, Jul. 2016, doi: 10.1007/S12591-016-0307-9.

[11] J. Ghosh, B. Sahoo, and S. Poria, "Prey-predator dynamics with prey refuge providing additional food to predator," *Chaos Solitons Fractals*, vol. 96, pp. 110–119, Mar. 2017, doi: 10.1016/J.CHAOS.2017.01.010.

[12] S. Khajanchi and S. Banerjee, "Role of constant prey refuge on stage structure predator–prey model with ratio-dependent functional response," *Appl Math Comput*, vol. 314, pp. 193–198, Dec. 2017, doi: 10.1016/J.AMC.2017.07.017.

[13] E. A. H. Jabr and D. K. Bahlool, "The Dynamics of a Food Web System: Role of a Prey Refuge Depending on Both Species," Iraqi Journal of Science, vol. 62, no. 2, pp: 639-657, 2021. doi: 10.24996/ijs.2021.62.2.29

[14] E. González-Olivares, B. González-Yañez, R. Becerra-Klix, and R. Ramos-Jiliberto, "Multiple stable states in a model based on predator-induced defences," *Ecological Complexity*, vol. 32, pp. 111–120, Dec. 2017, doi: 10.1016/J.ECOCOM.2017.10.004.

[15] M. Haque and S. Sarwardi, "Dynamics of a Harvested Prey–Predator Model with Prey Refuge Dependent on Both Species," *International Journal of Bifurcation and Chaos*, vol. 28, no. 12, Nov. 2018, doi: 10.1142/S0218127418300409.

[16] X. Wang, L. Zanette, and X. Zou, "Modelling the fear effect in predator-prey interactions," *J Math Biol*, vol. 73, no. 5, pp. 1179–1204, Nov. 2016, doi: 10.1007/S00285-016-0989-1.

[17] P. Panday, N. Pal, S. Samanta, and J. Chattopadhyay, "Stability and Bifurcation Analysis of a Three-Species Food Chain Model with Fear," *International Journal of Bifurcation and Chaos*, vol. 28, no. 1, Mar. 2018, doi: 10.1142/S0218127418500098.

[18] S. S. Nadim, S. Samanta, N. Pal, I. M. ELmojtaba, I. Mukhopadhyay, and J. Chattopadhyay, "Impact of Predator Signals on the Stability of a Predator–Prey System: A Z-Control Approach," *Differ Equ Dyn Syst*, vol. 30, no. 2, pp. 451–467, Apr. 2022, doi: 10.1007/S12591-018-0430-X.

[19] N. H. Fakhry, R. K. Naji, S. R. Smith?, and M. Haque, "Prey fear of a specialist predator in a tri-trophic food web can eliminate the superpredator," *Front Appl Math Stat*, vol. 8, Nov. 2022, doi: 10.3389/FAMS.2022.963991.

[20] A. R. M. Jamil and R. K. Naji, "Modeling and Analysis of the Influence of Fear on the Harvested Modified Leslie–Gower Model Involving Nonlinear Prey Refuge," *Mathematics*, vol. 10, no. 16, pp. 1–22, 2022, Accessed: Nov. 16, 2022. doi:10.3390/math10162857.

[21] Z. S. Abbas and R. K. Naji, "Modeling and Analysis of the Influence of Fear on a Harvested Food Web System," *Mathematics*, vol. 10, no. 18, Sep. 2022, doi: 10.3390/MATH10183300.

[22] F. Chen, "On a nonlinear nonautonomous predator–prey model with diffusion and distributed delay," *J Comput Appl Math*, vol. 180, no. 1, pp. 33–49, Aug. 2005, doi: 10.1016/J.CAM.2004.10.001.

[23] T. C. Gard, "Uniform persistence in multispecies population models," *Math Bio sci*, vol. 85, no. 1, pp. 93–104, Jul. 1987, doi: 10.1016/0025-5564(87)90101-5.

[24] L. Perko, "Differential Equations and Dynamical Systems," Springer, New York, 3rd edition, 2001, doi: 10.1007/978-1-4613-0003-8.

[25] H. K. Khalil, "Nonlinear Systems 3rd Edition ," *Prentice Hall*, 2002.